Reflectance of thin silver film on the glass substrate at the interaction with femtosecond laser pulses

2016 J. Phys.: Conf. Ser. 774 012099

(http://iopscience.iop.org/1742-6596/774/1/012099)

Reflectance of thin silver film on the glass substrate at the interaction with femtosecond laser pulses

Yu V Petrov[1,2], V A Khokhlov[1], N A Inogamov[1], K V Khishchenko[3] and S I Anisimov[1]

[1] Landau Institute for Theoretical Physics of the Russian Academy of Scienses, Akademika Semenova 1a, Chernogolovka, Moscow Region 142432, Russia
[2] Moscow Institute of Physics and Technology, Institutskiy Pereulok 9, Dolgoprudny, Moscow Region 141700, Russia
[3] Joint Institute for High Temperatures of the Russian Academy of Sciences, Izhorskaya 13 Bldg 2, Moscow 125412, Russia

E-mail: uvp49@mail.ru

Abstract. The optical response of thin silver film (of 60 nm thickness) coated on a glass prism (Kretschmann configuration) and heated by the femtosecond laser pulse of small intensity is investigated by the computational modeling. We have calculated the reflectance of p-polarized probe laser beam when it is incident onto the metal film from the glass side. Reflectance is calculated at incidence angles close to the surface plasmon resonance angle. We have considered first 100 ps after the action of femtosecond laser pulse onto the film surface. Changes in thermodynamic state and hydrodynamic motion of film material are described by the system of hydrodynamic equations taking into account different temperatures of electrons and ions (two-temperature state) and consequently two-temperature thermodynamics and kinetics at such early times. These changes define the changes in electron–ion and electron–electron collision frequencies. The collision frequencies of conduction electrons, being calculated in dependence on the density and electron and ion temperatures, allow us to find the Drude part of dielectric permittivity. Together with the interband contribution it gives possibility to calculate reflectance depending on the state of metal surface. It is shown a great importance of electron–electron interactions in the temporal behavior of reflectance at early times of laser–film interaction.

1. Introduction

Noble metals have significant conductivity because of their small electron–phonon collision frequencies. Because at low electron temperatures frequencies of electron–electron collisions are also minor, noble metals are best suited to investigate influence of electron–electron scattering on transport and optical properties of metals exposed to laser pulses of small intensity when a target matter remains solid. When considering optical properties of thin metal films surface plasmon technique [1–3] is widely used. We study the possibility of investigation of inner electron kinetics through the reflectivity measurements for the noble metal foil in connection with the surface plasmons.

2. Relaxation times of electron–ion and electron–electron collisions

Following the experimental situation, we consider reflection of probe laser pulse, passing through a glass prism, from a silver film coated on a prism (Kretschmann configuration) [4–6]. The

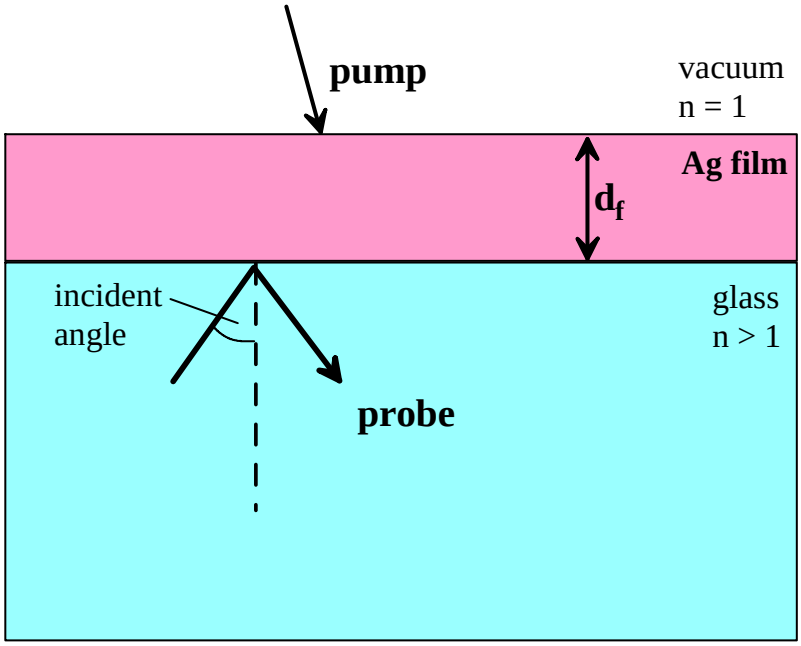

Figure 1. The scheme of experiment with Kretschmann configuration to measure the reflectivity by using the surface plasmon technique.

scheme of experiment is shown in figure 1. At the same time of the probe pulse action, previous femtosecond pump pulse of laser irradiation changing the state of metal film, acts onto its surface from the air–metal boundary. Laser irradiation fluence is substantially below the threshold of film melting, so metal remains solid.

We introduce permittivities in glass, metal and air respectively as $\epsilon_1, \epsilon_2, \epsilon_3$; $\epsilon_1 = 2.25$ and $\epsilon_3 = 1$ are real, while $\epsilon_2 = \epsilon_{21} + i\epsilon_{22}$. Real part ϵ_{21} and imaginary part ϵ_{22} of ϵ_2 are taken as a sum of corresponding Drude expressions $\epsilon_{D1}(x, T_e, T_i)$ and $\epsilon_{D2}(x, T_e, T_i)$ for intraband transitions, including dependence on the electron T_e and ion T_i temperatures and density and constant interband contributions b_1 and b_2:

$$\epsilon_{21}(x, T_e, T_i) = \epsilon_{D1}(x, T_e, T_i) + b_1, \quad \epsilon_{22}(x, T_e, T_i) = \epsilon_{D1}(x, T_e, T_i) + b_2, \tag{1}$$

$x = n/n_0$ is the relative concentration of atoms with respect to the concentration value at zero temperature and zero pressure (n_0 corresponds to the density 10.618 g/cc),

$$\epsilon_{D1}(x, T_e, T_i) = 1 - \omega_p^2(x)/(\omega^2 + \nu^2(x, T_e, T_i)), \tag{2}$$

$$\epsilon_{D2}(x, T_e, T_i) = \omega_p^2(x)\nu(x, T_e, T_i)/(\omega(\omega^2 + \nu^2(x, T_e, T_i))). \tag{3}$$

Plasma frequency squared

$$\omega_p^2(x) = \omega_p^2(x_r)(x/x_r), \tag{4}$$

where $\omega_p^2(x_r) = 4\pi z_s n_r e^2/m_s$, n_r is the concentration of atoms at the normal room conditions, $x_r = n_r/n_0$, $z_s = 1$ is the number of conduction (s) electrons per atom and m_s is their effective mass. Electron relaxation frequency $\nu(x, T_e, T_i) = \nu_{si}(x, T_i) + \nu_{se}(x, T_e)$, where ν_{si} and ν_{se} are frequencies of s-electron collisions with ions (electron–phonon collisions) and electrons (s–s and s–d collisions). Similar approach with the separation of Drude and interband contributions into

the dielectric permittivity of metals is used, for example, for Al in the work [7] and also for Ag in the work [8], where the asymptotic, quadratic in low electron temperatures, expression for electron–electron collision frequencies is extrapolated to more high temperatures of electrons.

In our approach, s–s and s–d-collision frequencies at different electron temperatures and concentration of atoms n_r were calculated in a similar way as it was done for the gold in our previous works [9]. According to data presented in [10] and to our calculations of electron band structure of silver [11, 12], we take values of the bottom of s-band, the lower bound of d-band and the upper bound of d-band at normal room conditions (temperature $T_\mathrm{r} = 293$ K, density $\rho_\mathrm{r} = 10.5$ g/cc) to be equal respectively to $\varepsilon_\mathrm{s} = -7.3$ eV, $\varepsilon_1 = -6.2$ eV, $\varepsilon_2 = -3.9$ eV (they are measured from the Fermi level which is equal to zero). Within the parabolic approximation of electron spectra in s- and d-bands with effective masses $m_\mathrm{s} = 0.75$ and $m_\mathrm{d} = 11.09$ in free electron mass units, it results in effective frequencies of s–d collisions $\nu_\mathrm{sd}(x, T_\mathrm{e})$ (in 10^{15} s^{-1}) which can be approximated by the expression

$$\nu_\mathrm{sd}(x, T_\mathrm{e}) = \left(\frac{10.618x}{10.5}\right)^{2/3} 8.54526 \frac{1 + 13.1307 t_\mathrm{e}^{2.24623}}{1 + 4.73045 t_\mathrm{e}^{2.92124}} \exp(-3.45232/t_\mathrm{e}), \tag{5}$$

where $t_\mathrm{e} = 6T_\mathrm{e}/(-\varepsilon_\mathrm{s} x^{2/3})$ and T_e is measured in eV. Analogously s–s collision frequency (also in 10^{15} s^{-1}) can be approximated by the formula

$$\nu_\mathrm{ss}(x, T_\mathrm{e}) = \left(\frac{10.618x}{10.5}\right)^{2/3} 0.982067 t_\mathrm{e}^2 \frac{1 + 0.237924 t_\mathrm{e}^{1.547}}{1 + 0.244546 t_\mathrm{e}^{2.62395}}. \tag{6}$$

Both s–d and s–s scatering in these formulas take into account normal e–e scattering processes.

To obtain dependence of s-electron–phonon collision frequency on the electron temperature and density, we proceed as previously [13, 14]. Electron mean free path due to the phonon scattering is taken as follows:

$$\lambda_\mathrm{si} \propto \frac{\theta^2(x)}{nT_\mathrm{i}} \propto \frac{\theta^2(x)}{xT_\mathrm{i}}, \tag{7}$$

where n is the concentration of atoms, $\theta(x)$ is the Debye temperature [13, 14]. To calculate dependence of Debye temperature on the density we introduce the approximation of cold pressure curve

$$p(x) = An_0 x(x^a - x^b) \tag{8}$$

with $a = 1.825$, $b = 1.755$, $A = 162$ eV. Then [13, 14],

$$\theta(x) \propto x^{1/3}\sqrt{y(x)}, \tag{9}$$

where

$$y(x) = \frac{(a+1)x^{2a+1}}{(b+1) + (a-b)x^{a+1}}. \tag{10}$$

It gives for the electron mean free path

$$\lambda_\mathrm{si} \propto \frac{y(x)}{x^{1/3}T_\mathrm{i}}, \tag{11}$$

and for the electron–phonon collision frequency

$$\nu_{\rm si}(x,T_{\rm i}) = \frac{v_{\rm F}}{\lambda_{\rm si}} \propto \frac{x^{2/3}T_{\rm i}}{y(x)}. \tag{12}$$

Here $v_{\rm F}$ is the Fermi velocity. Electron–phonon collision frequency at ordinary room conditions $\nu_{\rm si}(x_{\rm r},T_{\rm r})$ can be found by using the well known resistivity of silver at room conditions $\rho_{\rm r} = 15.87$ nOhm m from the Drude expression for resistivity

$$\nu_{\rm si}(x_{\rm r},T_{\rm r}) = \frac{n_{\rm r}e^2\rho_{\rm r}}{m_{\rm s}}. \tag{13}$$

Then for the electron–phonon collision frequency we obtain

$$\nu_{\rm si}(x,T_{\rm i}) = \nu_{\rm si}(x_{\rm r},T_{\rm r})\left(\frac{x}{x_{\rm r}}\right)^{2/3}\frac{y(x_{\rm r})}{y(x)}\frac{T_{\rm i}}{293} \tag{14}$$

with $T_{\rm i}$ measured in K.

Interband contributions into the dielectric permittivity, b_1 and b_2, can be found from the known value of the dielectric permittivity $\epsilon_2(x_{\rm r},T_{\rm r},T_{\rm r}) = \epsilon_{21}(x_{\rm r},T_{\rm r},T_{\rm r}) + {\rm i}\epsilon_{22}(x_{\rm r},T_{\rm r},T_{\rm r})$ at room temperature $T_{\rm r}$ in the one-temperature case with $\epsilon_{21}(x_{\rm r},T_{\rm r},T_{\rm r}) = -27.94$, $\epsilon_{22}(x_{\rm r},T_{\rm r},T_{\rm r}) = 1.51$ (we consider experiments with Ti:sapphire laser irradiation of wavelength 800 nm).

3. Reflectivity

On denoting z-components of wave vectors divided by the wave number k_3 in air as k_{1z}, k_{2z}, k_{3z} for transmitted light in the three substances correspondingly and $k^{\rm r}_{2z}$ for the reflected wave in the metal, the reflectivity can be written as

$$R = \left|\frac{R_1}{R_2}\right|^2 \tag{15}$$

with

$$R_1 = \left(k_{1z} - \frac{\epsilon_1}{\epsilon_2}k_{2z}\right)\left(k^{\rm r}_{2z} - \frac{\epsilon_2}{\epsilon_3}k_{3z}\right){\rm e}^{-{\rm i}k_{2z}k_3d_{\rm f}} + \left(k_{1z} - \frac{\epsilon_1}{\epsilon_2}k^{\rm r}_{2z}\right)\left(\frac{\epsilon_2}{\epsilon_3}k_{3z} - k_{2z}\right){\rm e}^{-{\rm i}k^{\rm r}_{2z}k_3d_{\rm f}}, \tag{16}$$

$$R_2 = \left(k_{1z} + \frac{\epsilon_1}{\epsilon_2}k_{2z}\right)\left(k^{\rm r}_{2z} - \frac{\epsilon_2}{\epsilon_3}k_{3z}\right){\rm e}^{-{\rm i}k_{2z}k_3d_{\rm f}} + \left(k_{1z} + \frac{\epsilon_1}{\epsilon_2}k^{\rm r}_{2z}\right)\left(\frac{\epsilon_2}{\epsilon_3}k_{3z} - k_{2z}\right){\rm e}^{-{\rm i}k^{\rm r}_{2z}k_3d_{\rm f}}. \tag{17}$$

Here $d_{\rm f}$ is the foil thickness. Introducing the incidence angle α, we have

$$k_{1x} = \sqrt{\epsilon_1}\sin\alpha, \quad k_{1z} = \sqrt{\epsilon_1}\cos\alpha, \quad k_{2z} = k_{21} + {\rm i}k_{22}, \quad k^{\rm r}_{2z} = k_{21} - {\rm i}k_{22}, \quad k_{3z} = \sqrt{\epsilon_3 - k^2_{1x}}, \tag{18}$$

with

$$k_{21} = \sqrt{\frac{1}{2}\left(\sqrt{\left(\epsilon_{21} - k^2_{1x}\right)^2 + \epsilon^2_{22}} + \epsilon_{21} - k^2_{1x}\right)}, \tag{19}$$

$$k_{22} = \sqrt{\frac{1}{2}\left(\sqrt{\left(\epsilon_{21} - k^2_{1x}\right)^2 + \epsilon^2_{22}} - \epsilon_{21} + k^2_{1x}\right)}. \tag{20}$$

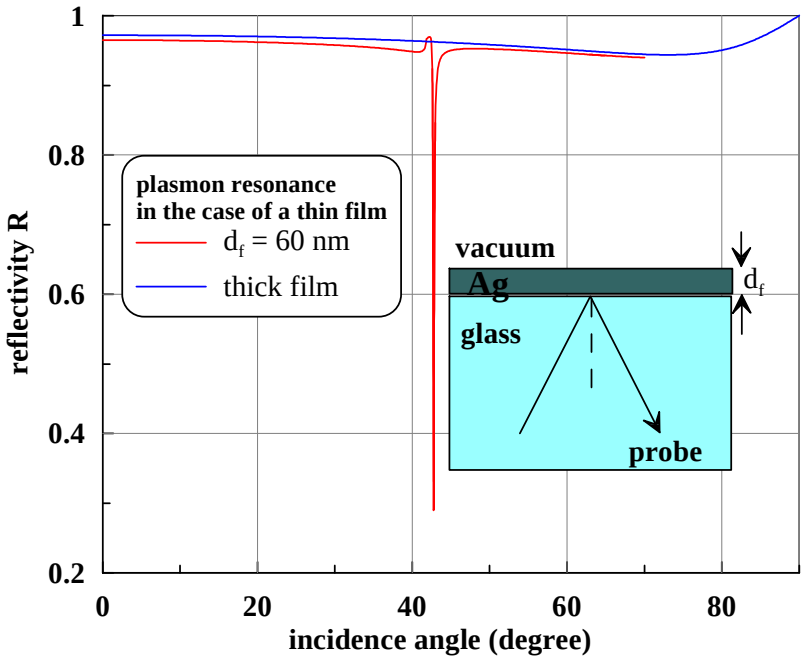

Figure 2. Reflectivity of a 60 nm silver foil coated on a glass in Kretschmann configuration as a function of incidence angle. Wavelength of light is 800 nm. Absorbed fluence value is $F = 0.7$ mJ/cm^2. The minimum reflectivity corresponds to the surface plasmon resonance. Plasmon resonance angle is 42.78°.

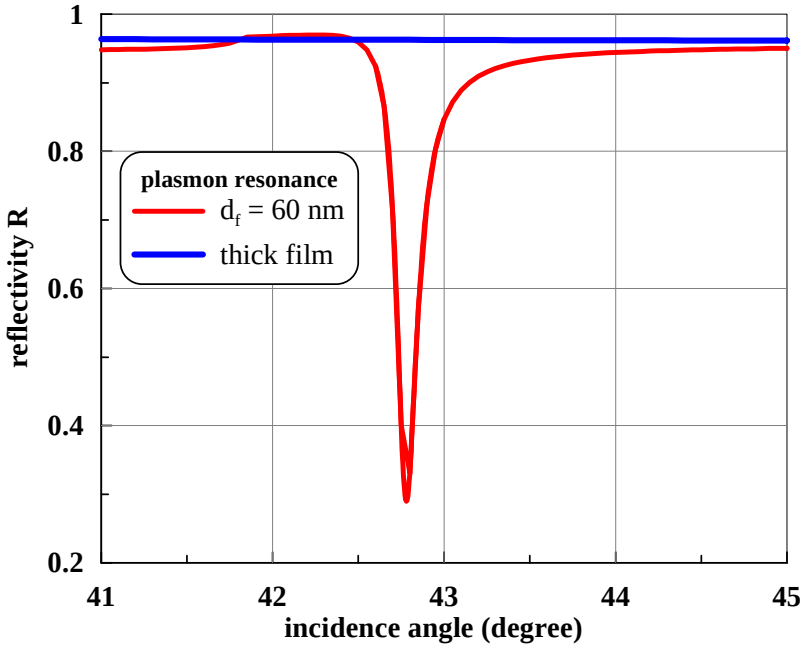

Figure 3. More detailed reflectivity of silver in Kretschmann configuration at angles of incidence close to the surface plasmon resonance angle.

In figures 2 and 3, reflectivity at room conditions is shown as a function of angle of incidence and exhibits surface plasmon resonance at angles close to 42.78°.

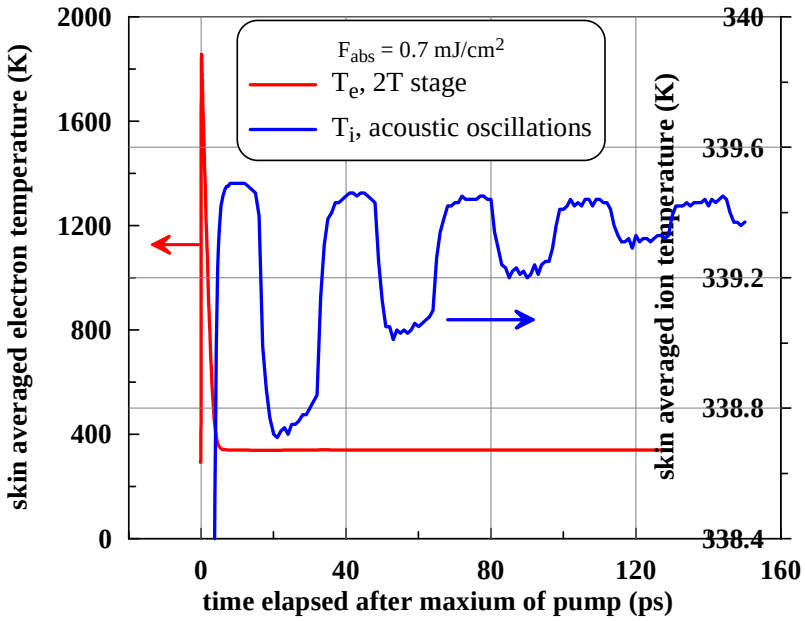

Figure 4. Temporal change of electron and ion temperatures in silver foil under the action of laser pump.

Dynamics of motion of a target matter and change of its state under the action of pump femtosecond laser pulse can be described by the system of hydrodynamic equations [15, 16]. These are one-dimensional equations because of the small foil thickness (60 nm) in comparison with the size of the laser spot (few tenth of mm). Used hydrodynamic equations take into account two-temperature character of state of matter with unequal temperatures of electrons and ions, electron–ion energy exchange, electron thermal conductivity, they describe the occurrence of shift elastic stress during the movement of a target matter. In figure 4 the change of the electron and ion temperatures due to the laser irradiation obtained from the solution of hydrodynamic equations is shown depending on time for the value of the absorbed fluence $F = 0.7$ mJ/cm^2.

We consider angles of incidence of probe pulse to be close to the surface plasmon resonance angle. Then for temporal Gaussian type pump pulse according to the system of hydrodynamic equations we find density, electron and ion temperatures of silver foil and consequently reflectivity depending on time. Interesting in the difference between the reflectivity of foil heated by the laser pulse and reflectivity of undisturbed target, we can change angle of incidence of the probe pulse to achieve the most noticeable effect. Figures 5–7 show temporal evolution of the reflectivity for the value of absorbed fluence $F = 0.7$ mJ/cm^2 at different values of angles of incidence. Significant drop of reflectivity at small times is connected with the rapid increase of the electron temperature in figure 4 while the following oscillations are due to film acoustical vibrations (oscillation period is consistent with the value $T = 2d_\mathrm{f}/c_S$, where $d_\mathrm{f} = 60$ nm is the foil thickness and $c_S = 3.65$ km/s is the sound velocity of silver). In figure 8 results of our calculations of the temporal behavior of reflectivity are compared with the experimental results done in the work [5]. In both cases the angle of incidence 0.5° exceeds the surface plasmon resonance angle. Similar good agreement of both experimental and theoretical results as for the time location as for the value of relative change of reflectivity takes place so for another two values of deflection of incidence angle from a resonance value: −2° and +2.5°.

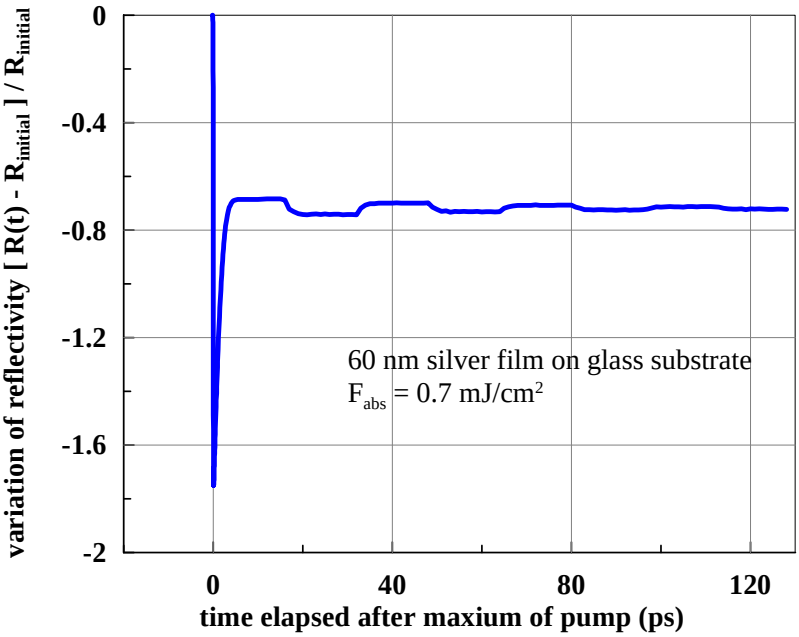

Figure 5. Relative change of reflectance of 60 nm silver coated on a glass (in percent) when the incidence angle is only 0.5° more than the surface plasmon resonance angle. Absorbed fluence is $F = 0.7$ mJ/cm^2. Sharp drop of reflectance is due to the sharp increase of the electron temperature under the action of ultrashort laser pump-pulse.

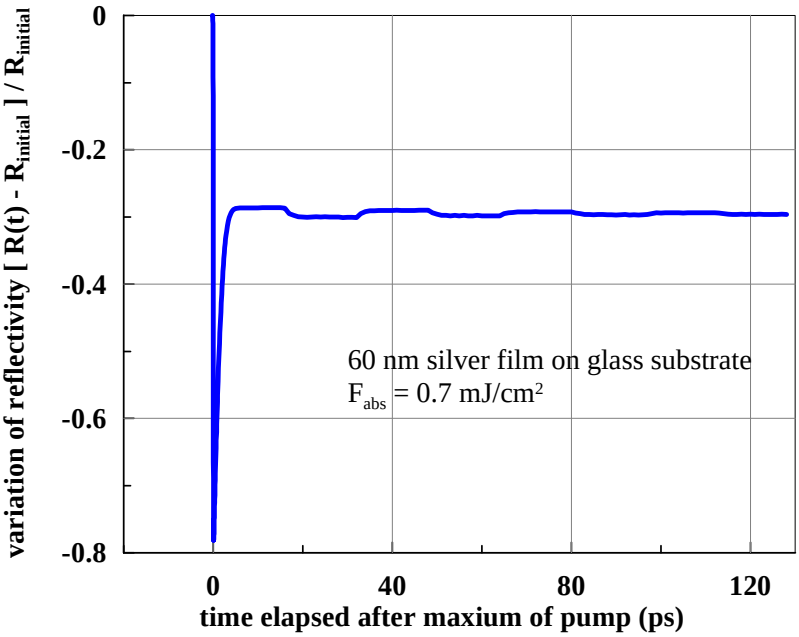

Figure 6. Temporal change (in percent) of the relative reflectance of 60 nm silver on a glass. Angle of incidence is taken to be 2° less than the surface plasmon resonance angle. Sharp drop of reflectance shows smaller value than when the incidence angle is close to the angle of plasmon resonance.

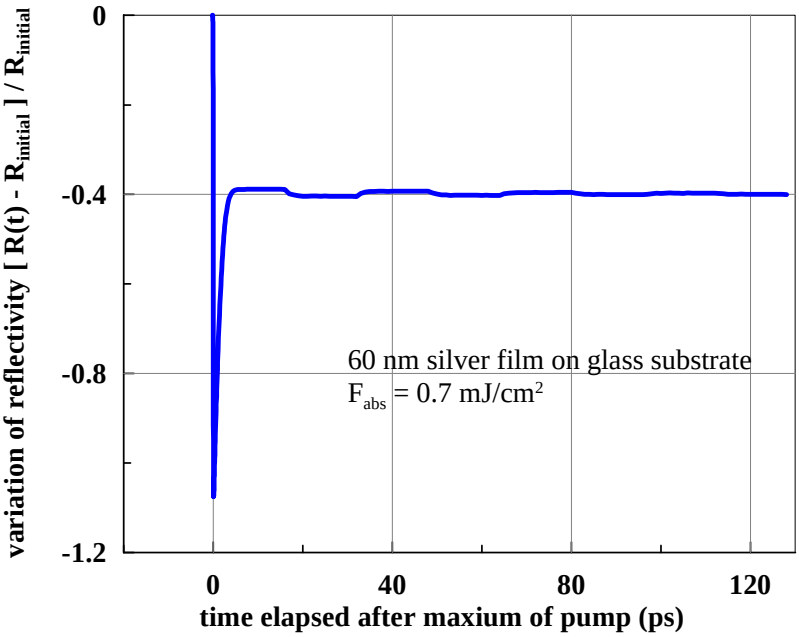

Figure 7. Time-dependent change (in percent) of the relative reflectance of 60 nm silver on a glass when the incidence angle is 2.5° more than the surface plasmon resonance angle. Magnitude of a sharp fall of reflectance is smaller than in the case when the incidence angle is close to the resonance angle.

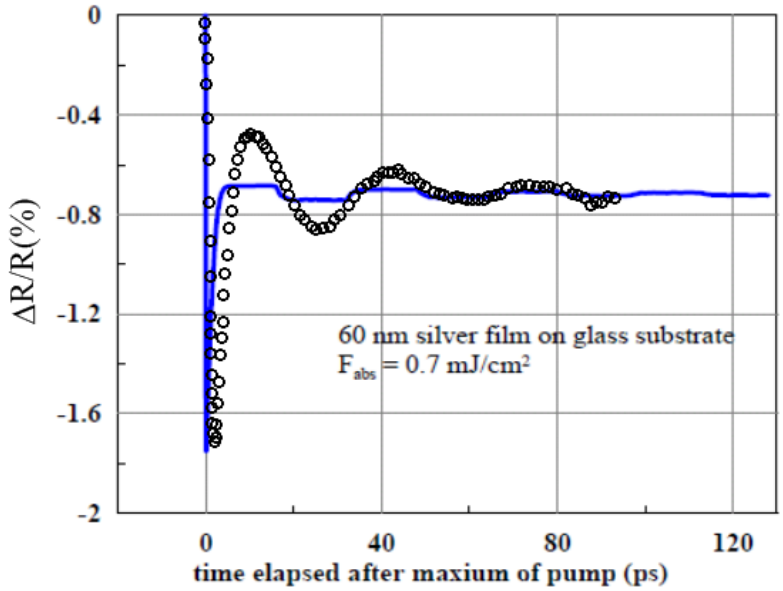

Figure 8. Comparison of the theoretical and experimental values of the relative change of reflectance of 60 nm silver on a glass (in percent) at the incidence angle 0.5° more than the surface plasmon resonance angle. Solid line presents the results of our theoretical calculations, circles are experimental values obtained in the work [5].

4. Conclusion

We have considered the influence of the fast isochoric heating of the electron subsystem of a noble metal (silver) onto the initial change of the thermodynamic and optical properties of metal in the geometry of thin film coated onto the glass substrate. For the best observations of the optical transformations in a metal a theory related to the surface plasmon excitation is used. Dielectric permittivity applied takes into account Drude intraband transitions of conduction electrons with electron–phonon collisions, characteristic for solid state of noble metals and electron–electron collisions increasing with the electron temperature increase. Electron–electron collisions include s–s and s–d scattering with frequencies calculated in the framework of relaxation time approach. In addition interband transitions are included to contribute to the dielectric permittivity. Strong change of the reflectivity near the incidence angle of surface plasmon resonance at first picoseconds of the laser–matter interaction, due to the large increase of the electron temperature, is fixed well in our calculations. These calculations are based upon the investigation of hydrodynamic motion of matter and change of its thermodynamical and optical state. Our theoretical calculations agree well with the results of appropriate experimental investigations.

Acknowledgments

This work is partially supported by grants from the Russian Foundation for Basic Research (No. 16-02-00864) and the President of the Russian Federation (No. NSh-10174.2016.2).

References

[1] van Exter M and Lagendijk A 1988 *Phys. Rev. Lett.* **60** 49–52
[2] Groeneveld R H M, Sprik R and Lagendijk A 1990 *Phys. Rev. Lett.* **64** 784–787
[3] Temnov V V 2012 *Nature Photon.* **6** 728–736
[4] Sambles J R, Bradbery G W and Yang F 1991 *Contemp. Phys.* **32** 173
[5] Wang J and Guo C 2013 *Appl. Phys.* A **111** 273–277
[6] Wang J and Guo C 2007 *Phys. Rev.* B **75** 184304
[7] Agranat M B, Andreev N E, Ashitkov S I, Veysman M E, Levashov P R, Ovchinnikov A V, Sitnikov D S, Fortov V E and Khishchenko K V 2007 *JETP Lett.* **85** 271–276
[8] Veysman M E, Agranat M B, Andreev N E, Ashitkov S I, Fortov V E, Khishchenko K V, Kostenko O F, Levashov P R, Ovchinnikov A V and Sitnikov D S 2008 *J. Phys.* B **41** 125704
[9] Petrov Yu V, Inogamov N A and Migdal K P 2013 *JETP Lett.* **97** 20–27
[10] Babar S and Weaver J H 2015 *Appl. Opt.* **54** 477–481
[11] Migdal K P, Il'nitsky D K, Petrov Yu V and Inogamov N A 2015 *J. Phys.: Conf. Ser.* **653** 012086
[12] Petrov Yu V, Migdal K P, Inogamov N A and Zhakhovsky V V 2015 *Appl. Phys.* B **119** 401–411
[13] Petrov Yu V, Inogamov N A, Anisimov S I, Migdal K P, Khokhlov V A and Khishchenko K V 2015 *J. Phys.: Conf. Ser.* **653** 012087
[14] Petrov Yu V, Inogamov N A and Migdal K P 2015 *Progress in Electromagnetics Research Symp. Proc.* (PIERS) pp 2431–2435
[15] Inogamov N A, Zhakhovsky V V, Petrov Yu V, Khokhlov V A, Ashitkov S I, Khishchenko K V, Migdal K P, Ilnitsky D K, Emirov Yu N, Komarov P S, Shepelev V V, Miller C W, Oleynik I I, Agranat M B, Andriyash A V, Anisimov S I and Fortov V E 2013 *Contr. Plasma Phys.* **53** 796–810
[16] Khokhlov V A, Inogamov N A, Zhakhovsky V V, Shepelev V V and Il'nitsky D K 2015 *J. Phys.: Conf. Ser.* **653** 012003